scientific reports

Check for updates

OPEN

Upregulation of ELP3 in acinar cells during acute pancreatitis is dispensable for homeostasis, inflammation, regeneration, and cancer initiation

Elias Aajja[1✉], Hélène Lefort[1], Siam Mahibullah[1], Marine Leclercq[2], Katherine J. Aney[6,7,8,9], Sahar Nissim[6,7,8,9,10], Laurent Nguyen[3,5], Alain Chariot[4,5], Patrick Henriet[1], Donatienne Tyteca[1], Pierre Close[2,5,11✉] & Christophe E. Pierreux[1,11✉]

Pancreatitis, or inflammation of the pancreas, is a common gastrointestinal condition. While often acute and self-resolving, it can become chronic and promote pancreatic ductal adenocarcinoma (PDAC), the third deadliest cancer worldwide. Pancreatitis is accompanied by morphological and molecular changes, notably immune cell infiltration, fibrosis, and acinar-to-ductal metaplasia (ADM). ELP3, the catalytic subunit of the Elongator complex, modifies wobble uridine tRNAs to optimize codon translation rates. It is critical to inflammatory processes and cancer in multiple organ systems, yet its role in the pancreas has not been investigated. This study aimed to investigate the expression and implication of ELP3 during pancreatitis induced in mice via repetitive caerulein injections. Acute pancreatitis was accompanied by increased expression of ELP3, which was mainly detected in pancreatic epithelial cells. To assess its function, we genetically inactivated *Elp3* in pancreatic epithelial cells. *Elp3* deficiency had no detectable effects on pancreas homeostasis, on the initiation and resolution of acute pancreatitis, on the development of chronic pancreatitis, or on pancreatitis-induced PDAC initiation. Our findings indicate that ELP3 is dispensable in pancreatic formation, inflammation and PDAC initiation. Future studies should explore its role in non-epithelial cells and its potential involvement in other PDAC hallmarks, such as therapy resistance.

Acute pancreatitis is a prevalent gastrointestinal condition characterized by rapid and transient inflammation of the pancreas. Its most common causes are associated with a Western lifestyle, including gallstones, heavy alcohol consumption, and hypertriglyceridemia[1–3]. While many patients recover, acute pancreatitis can have a high mortality rate due to widespread severe inflammation and a systemic cytokine storm[4]. In some cases, the disease progresses to walled-off necrosis, a severe and clinically challenging complication characterized by encapsulated areas of pancreatic and peripancreatic tissue necrosis[4]. Even in patients who survive acute pancreatitis, long-term complications may arise, including chronic pancreatitis, pancreatic insufficiency, diabetes mellitus, or pancreatic cancer[5]. Notably, pancreatitis is a well-established risk factor for pancreatic ductal adenocarcinoma (PDAC), the most common and lethal form of pancreatic cancer. This relationship underscores the need to understand how acute inflammation progresses into chronic disease and contributes to oncogenesis.

[1]Cell Biology Unit, de Duve Institute, Université Catholique de Louvain, 1200 Woluwé-Saint-Lambert, Belgium. [2]Laboratory of Cancer Signaling, GIGA Institute, Université de Liège, 4000 Liège, Belgium. [3]Laboratory of Molecular Regulation of Neurogenesis, GIGA Institute, Université de Liège, 4000 Liège, Belgium. [4]Laboratory of Cancer Biology, GIGA Institute, Université de Liège, 4000 Liège, Belgium. [5]Walloon Excellence in Life Sciences and Biotechnology, WEL Research Institute, 1300 Wavre, Belgium. [6]Biological and Biomedical Sciences Program, Harvard Medical School, Boston, MA, USA. [7]Health Sciences and Technology Program, Harvard-MIT, Boston, MA, USA. [8]Genetics Division, Brigham and Women's Hospital, Harvard Medical School, Boston, MA, USA. [9]Dana-Farber Cancer Institute, Boston, MA, USA. [10]Gastroenterology Division, Brigham and Women's Hospital, Harvard Medical School, Boston, MA, USA. [11]Pierre Close and Christophe E. Pierreux contributed equally to this work. ✉email: elias.aajja@uclouvain.be; pierre.close@uliege.be; christophe.pierreux@uclouvain.be

Acute pancreatitis is triggered by the premature activation of digestive enzymes, which are continuously produced in abundance by acinar cells to fulfill the exocrine glandular function of the pancreas. This premature enzyme activation results in pancreatic autodigestion and acinar cell death. This process triggers an inflammatory cascade and causes pancreatic tissue remodeling[1–3]. Three major histopathological and morphological changes characterize acute pancreatitis: immune cell infiltration, extracellular matrix remodeling and fibrosis, and acinar-to-ductal metaplasia (ADM)[6–9]. ADM is a process by which acinar cells transdifferentiate into ductal-like cells, thereby producing less digestive enzymes and likely serving as a protective mechanism against further enzymatic damage. These ductal-like cells are proliferative and can revert back to the acinar phenotype, potentially aiding pancreatic regeneration following injury[8,10,11]. However, persistent ADM in the presence of unresolved inflammation can lead to PDAC initiation[12]. This highlights the balance between regeneration and disease progression.

ELP3 is the catalytic subunit of the Elongator complex, a six-subunit acetyltransferase complex (ELP1-6) highly conserved in eukaryotes[13–16]. Initially identified as a histone acetyltransferase (HAT) involved in transcriptional elongation[17–19], Elongator was later found to mainly function in the cytoplasm[20], primarily acting as a tRNA-modifying complex[21,22]. Additionally, Elongator interacts with microtubules, and its loss of activity impairs α-tubulin acetylation, thereby interfering with radial migration, branching, maturation, and differentiation of cortical projection neurons[22,23]. A central role of Elongator is to enhance translation efficiency by modifying wobble uridine of transfer RNAs (tRNAs) with a carboxymethyl group at the C5 position[24]. Two other enzymes, the cytoplasmic thiouridylases 1 and 2 (CTU1 and CTU2), catalyze the addition of a thiol group at the C2 position of wobble uridine, leading to the fully modified 5-methoxycarbonylmethyl-2-thiouridine-34 ($mcm^5s^2U_{34}$) form, which ensures proper codon-anticodon interactions and translational optimization of NAA-enriched mRNAs (NAA refers to codons composed of any nucleotide followed by two adenines: N = any nucleotide, A = adenine)[25].

Elongator, through its ability to modify the wobble uridine of tRNAs, has been implicated in multiple diseases and conditions. These discoveries have been made possible thanks to ELP3 knockout models. In colon cancer, ELP3 regulates SOX9 translation in an NAA-dependent manner, maintaining $Lgr5^+$/$Dclk1^+$/$Sox9^+$ cells, which are essential for tumor development[26]. In breast cancer, ELP3 regulates DEK proto-oncogene translation, which in turn promotes internal ribosome entry site (IRES)-dependent translation of Lymphoid enhancer-binding factor 1 (LEF1), a transcription factor that promotes tumor invasion and metastasis[27]. In melanoma, ELP3 enhances resistance to anti-BRAF therapy by promoting the translation of Hypoxia-inducible factor 1-alpha (HIF1α)[28]. Beyond cancer, ELP3 loss triggers an amino acid deprivation-like response, leading to Activating transcription factor 4 (ATF4) overactivation and widespread effects on cellular differentiation. In hematopoietic progenitors, this response activates a protein 53 (p53)-dependent antitumor checkpoint, resulting in hematopoietic failure[29]. In T follicular helper cells, excessive ATF4 signaling impairs activation, proliferation, and differentiation[30]. In intestinal epithelial cells, ELP3 loss restricts the amplification and differentiation of tuft cells[31]. ELP3 also plays a key role in inflammation. Its inactivation exacerbates colitis by promoting pro-inflammatory/classical macrophage differentiation[32]. Conversely, ELP3 is induced by interleukins 4 and 13 (IL-4 and IL-13) in macrophages, where it promotes alternative/anti-inflammatory macrophage polarization through codon-dependent regulation of Resistance to inhibitors of cholinesterase-8B (Ric8b), a mammalian target of rapamycin complex 2 (mTORC2) activator[32]. Thus, the role of ELP3 is context-dependent across different cell types and tissues, influencing cancer progression, immune regulation, and cellular differentiation.

Despite being extensively studied in various contexts, the expression and function of ELP3 in pancreatic physiological and pathological conditions, including acute pancreatitis, remain unexplored. Given ELP3's crucial roles in inflammation, cell-fate regulation, and tumor initiation in other tissues, we hypothesized that it could likewise play a role in acute pancreatitis and the early events of PDAC initiation. Investigating ELP3 in acute pancreatitis is particularly relevant as this condition involves macrophage polarization[33], and differentiation processes such as ADM[8], which ELP3 may regulate. Additionally, ELP3 plays a role in colon cancer initiation, raising the question of whether it may also influence pancreatic tumorigenesis through acute pancreatitis. To address these knowledge gaps, we used a mouse model of acute pancreatitis to examine the expression and function of ELP3. We then employed pancreatic epithelial- and acinar-specific *Elp3* knockout mice to dissect the mechanism through which ELP3 may contribute to acute pancreatitis. Furthermore, because of broad cell/tissue specific roles of ELP3, there is a need to investigate its roles in pancreatic epithelial cells specifically to distinguish their functions from the non-epithelial compartment. Contrary to our initial hypothesis, we found that while ELP3 expression is upregulated during acute pancreatitis, its epithelial-specific deletion had no impact on the initiation or regeneration of acute pancreatitis, chronic pancreatitis, and PDAC initiation. By demonstrating that ELP3 is dispensable in epithelial cells during pancreatitis and tumor initiation, we refine the understanding of ELP3's tissue-specific functions and highlight the importance of studying regulators in a context-dependent manner using cell-type specific, inducible models.

Results

Acute pancreatitis is associated with upregulated ELP3 expression in metaplastic cells

Acute pancreatitis was induced in C57BL/6 N mice by six caerulein injections every other day over three injection days, and pancreatic tissues were collected one day after the final injection (day 6; Fig. 1A). Histological analysis with hematoxylin & eosin staining revealed extensive and profound pancreatic tissue remodeling, as expected (Fig. 1B). In control pancreata, the pyramidal acinar cells were densely packed, and their apical secreting poles filled with zymogen granules exhibited strong eosinophilia that gave the tissue its characteristic pink appearance (Fig. 1B). Following caerulein injections, global pancreatic eosinophilia decreased (Fig. 1B), consistent with reduced acinar density and decreased zymogen granule content in the remaining cells due to ADM. Meanwhile, basophilia increased in the interstitial spaces (Fig. 1B), likely reflecting immune cell infiltration and fibrosis.

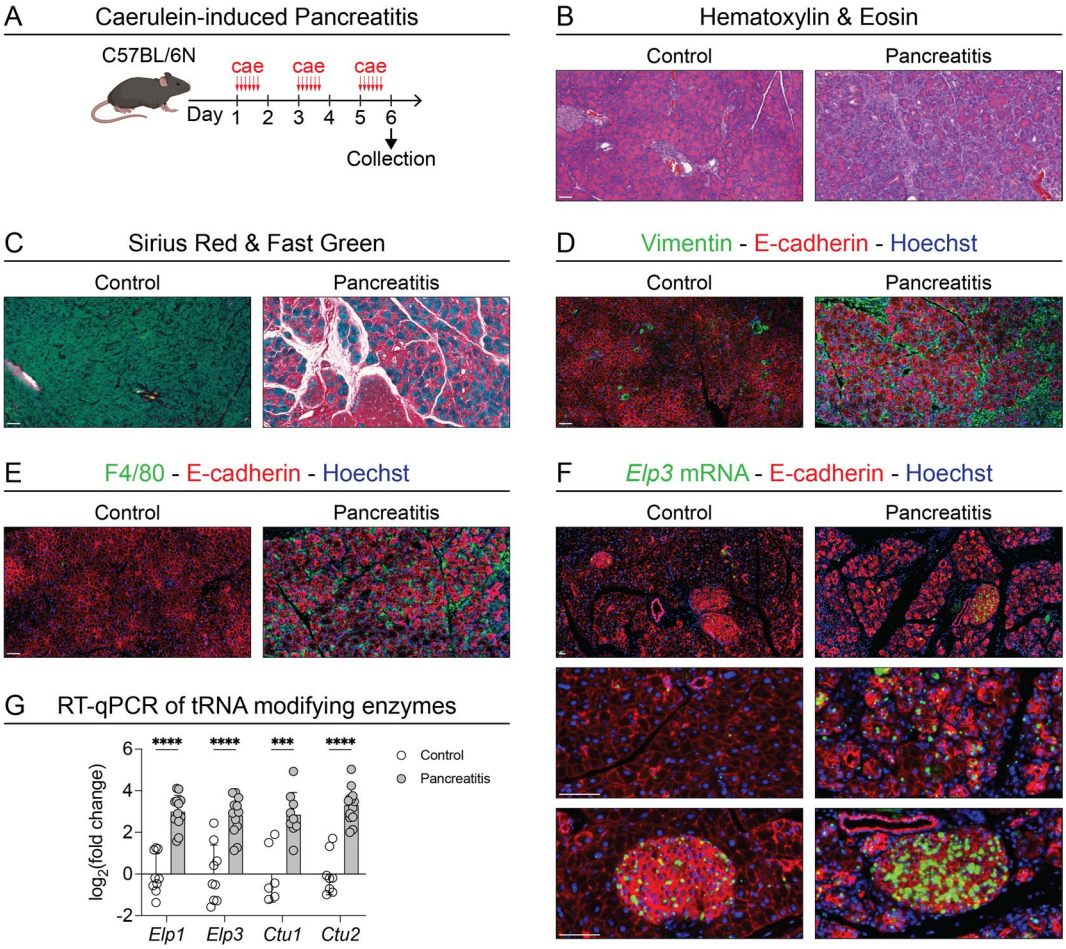

Fig. 1. ELP3 expression in the pancreas and acute pancreatitis. (**A**) Experimental timeline of acute pancreatitis showing caerulein injections and tissue collection one day after the final injection (day 6) in C57BL/6 N mice. Vertical red arrows indicate the hourly injections. (**B,C**) Pancreatic tissue staining: (B) hematoxylin & eosin staining of nuclei (hematoxylin) and cytoplasm/extracellular matrix (eosin), and (C) sirius red/fast green staining of collagen fibers (sirius red) and cytoplasm (fast green), in control and caerulein-treated mice. Scale bar: 50 µm. (**D,E**) Immunofluorescence labeling of pancreatic sections for vimentin & E-cadherin (D), and for F4/80 & E-cadherin (E), to visualize fibroblasts (vimentin), macrophages (F4/80), and epithelial cells (E-cadherin), with Hoechst nuclear counterstaining, in control and caerulein-treated mice. Scale bar: 50 µm. (**F**) *Elp3* mRNA in situ hybridization using RNAscope™ combined with immunofluorescence labeling for E-cadherin (epithelial cells), and Hoechst nuclear counterstaining, in control and caerulein-treated mice. Scale bar: 50 µm. (**G**) RT-qPCR analysis of *Elp1*, *Elp3*, *Ctu1*, and *Ctu2* expression in pancreatic tissue from control and caerulein-treated mice and normalized to *18 S* ribosomal RNA. Data are mean ± SD. Statistical significance was determined by two-tailed Student's t-test. $^{*}p < 0.05$, $^{**}p < 0.01$, $^{***}p < 0.001$, $^{****}p < 0.0001$. $n \geq 7$.

Sirius red/fast green staining further confirmed these histological changes. Acini, which stained green with fast green, appeared reduced in size, consistent with observations from hematoxylin & eosin staining (Fig. 1C, compare green in Fig. 1C with pink in Fig. 1B). Sirius red, which stains collagen fibers, showed a marked increase following caerulein injections, indicative of fibrosis (Fig. 1C). Labeling of vimentin, a fibroblast marker, and E-cadherin, an epithelial marker, confirmed a reduction in acinar compartment size during pancreatitis and revealed an increased presence of fibroblasts between the acini, indicative of fibrosis (Fig. 1D). Similarly, immunofluorescence of F4/80, a macrophage marker, and E-cadherin revealed diminished acinar area with significant macrophage infiltration in the surrounding spaces (Fig. 1E). The observed reduction in acinar area is likely a consequence of caerulein-induced injury and acinar-to-ductal metaplasia (ADM). Collectively, these results demonstrate that our model of repetitive caerulein injections successfully recapitulates the histopathological features of acute pancreatitis.

Given that this model faithfully recapitulates key features of acute pancreatitis, we then sought to study the expression of ELP3 in this context. To this end, we employed RNAscope™ in situ hybridization to visualize and identify in the pancreatic tissue the *Elp3* mRNA expressing cells (Fig. 1F). In control pancreata, *Elp3* mRNA was predominantly expressed in endocrine cells within the islets of Langerhans (Fig. 1F, lower panels). However, during acute pancreatitis, *Elp3* mRNA expression increased in endocrine cells but also in non-endocrine epithelial cells, including acinar cells, which are expected to undergo ADM in this condition (Fig. 1F, middle

panels). RT-qPCR analysis further confirmed the upregulation of *Elp3* mRNA, along with its associated genes, including Elongator complex Protein 1 *Elp1* and the cytoplasmic thiouridylases *Ctu1* and *Ctu2* (Fig. 1G). Single-cell RNA sequencing further confirmed that *Elp1–6* and *Ctu1/2* were upregulated in both epithelial and acinar/ADM cells during acute pancreatitis (Supplementary Fig. 1)[34]. These findings indicate that ELP3 expression, along with its associated components, is upregulated during acute pancreatitis. An increase in *Elp3* expression was also observed in non-epithelial cells, including macrophages and, most prominently, pancreatic stellate cells, based on publicly available single-cell RNA-sequencing data (Supplementary Fig. 2). This pattern was further confirmed by in situ hybridization in our model (Supplementary Fig. 2), indicating that Elp3 upregulation during inflammation is not restricted to the epithelium, but occurs across multiple pancreatic cell types.

Epithelial-specific *Elp3* inactivation is dispensable for acute pancreatitis

To investigate the role of ELP3 in acute pancreatitis, we specifically inactivated *Elp3* in pancreatic epithelial cells (PECs), where *Elp3* expression was upregulated (Fig. 1F), by generating $Elp3^{\Delta PEC}$ mice. This was achieved by crossing Pdx1-Cre mice with $Elp3^{fl/fl}$ mice, to obtain the *Pdx1-Cre;* $Elp3^{fl/fl}$ genotype, here referred to as $Elp3^{\Delta PEC}$, in the second generation. In these mice, the Cre recombinase is constitutively expressed in Pdx1-positive common pancreatic progenitor thanks to Pdx1 regulatory elements. Cre-mediated recombination induces a frameshift deletion of *Elp3* exon 2 (*Elp3-E2*), resulting in the specific knockout of *Elp3* in all PECs. $Elp3^{\Delta PEC}$ were compared to their $Elp3^{WT}$ littermates (Fig. 2A). BaseScope™ in situ hybridization confirmed that *Elp3-E2* mRNA was absent in pancreatic epithelial cells in $Elp3^{\Delta PEC}$ pancreatitis, as compared to $Elp3^{WT}$ littermates (Supplementary Fig. 1).

Macroscopic analysis revealed no significant differences between $Elp3^{\Delta PEC}$ and $Elp3^{WT}$ pancreata under both control and acute pancreatitis conditions (Fig. 2B). Whole-slide scans were used for all histological analyses to ensure unbiased assessment across the entire tissue. Histological examination using hematoxylin & eosin staining of full pancreatic sections scanned showed no major differences between control $Elp3^{\Delta PEC}$ and $Elp3^{WT}$ pancreata. Similarly, both $Elp3^{\Delta PEC}$ and $Elp3^{WT}$ mice exhibited comparable histopathological features following acute pancreatitis (Fig. 2C). Immunofluorescence labeling of F4/80, vimentin, and E-cadherin demonstrated similar levels of macrophages, fibroblasts and epithelial density in both $Elp3^{\Delta PEC}$ and $Elp3^{WT}$ acute pancreatitis, suggesting that epithelial *Elp3* deletion does not affect the development of acute pancreatitis in response to caerulein (Fig. 2D-E).

We then performed bulk RNA sequencing on $Elp3^{\Delta PEC}$ and $Elp3^{WT}$ pancreata under both control and acute pancreatitis conditions. The transcriptomic analysis allowed us to investigate the molecular and cellular effects of *Elp3* loss in both healthy and inflamed pancreata. RNA sequencing data revealed the appearance and increase in *Elp3* mRNA read counts that skipped exon 2 in $Elp3^{\Delta PEC}$ mice compared to $Elp3^{WT}$ littermates, indicating that recombination had occurred (Supplementary Fig. 1). Volcano plots comparing pancreatitis versus control conditions revealed a similar number of differentially expressed genes in $Elp3^{\Delta PEC}$ and $Elp3^{WT}$ mice (Fig. 3A, left), with most of the genes being shared (Fig. 3B), suggesting that *Elp3* inactivation in PECs did not impact acute pancreatitis and the overall response to caerulein-induced injury. Likewise, direct comparisons between $Elp3^{\Delta PEC}$ and $Elp3^{WT}$ pancreata, in both control and pancreatitis conditions, showed minimal transcriptional differences, further suggesting that epithelial *Elp3* inactivation had little impact under either condition (Fig. 3A, right). The Venn diagram reinforced this by showing that most differentially expressed genes in the pancreatitis versus control comparison for both $Elp3^{\Delta PEC}$ and $Elp3^{WT}$ were shared, while fewer were unique to either genotype, and only a small number of genes were found in the direct $Elp3^{\Delta PEC}$ versus $Elp3^{WT}$ comparisons (Fig. 3B). Heatmaps of immune infiltration, fibrosis, acinar, and ductal genes further supported the absence of effect of ELP3 in pancreatitis. Indeed, the expression of genes dramatically impacted by pancreatitis were not affected by the absence of ELP3 in the pancreas (Fig. 3C). Gene ontology (GO) analysis further confirmed these observations, with a substantial overlap in differentially regulated pathways in the pancreatitis versus control comparisons in both $Elp3^{\Delta PEC}$ and $Elp3^{WT}$ mice, and no distinct signature differentiating $Elp3^{\Delta PEC}$ from $Elp3^{WT}$, in both healthy and inflamed pancreata (Fig. 3D, Venn diagram). As expected, GO enrichment analysis highlighted inflammation-related pathways as the primary transcriptional response to pancreatitis in $Elp3^{\Delta PEC}$ and $Elp3^{WT}$ mice, with signatures associated with immune cell infiltration and fibrosis being the most prominent (Fig. 3D, bubble plot). Yet, these signatures remained unchanged between $Elp3^{\Delta PEC}$ and $Elp3^{WT}$ mice (Fig. 3D, bubble plot).

Together, these findings indicate that while acute pancreatitis is associated with increased ELP3 expression in pancreatic epithelial cells, its role is dispensable, since the morphology, histology, and bulk transcriptome of both healthy and inflamed pancreata are not impacted in the $Elp3^{\Delta PEC}$ mice.

Epithelial-specific *Elp3* inactivation is dispensable for regeneration following acute pancreatitis

Since pancreatic epithelial ELP3 was not required for the initiation and development of acute pancreatitis, we next evaluated its role in pancreatic regeneration after caerulein-induced injury. To do so, we collected pancreata at three (day 8) and five days (day 10) after the final caerulein injection (Fig. 4A), at which point the elevated expression of U_{34}-tRNA-modifying enzymes persisted in $Elp3^{WT}$ mice (Supplementary Fig. 2).

Histological analysis using hematoxylin & eosin staining showed comparable tissue architecture between $Elp3^{\Delta PEC}$ and $Elp3^{WT}$ mice during recovery, with both groups exhibiting progressive recovery of the epithelial architecture with acinar expansion demonstrated by a clear increase in global tissue eosinophilia five days after the final caerulein injection, returning to a state resembling the control condition (Fig. 4B, compare with Fig. 2C, control). Similarly, immunofluorescence labeling of F4/80, vimentin, and E-cadherin revealed no differences in macrophage presence, fibroblast levels, or epithelial density between $Elp3^{\Delta PEC}$ and $Elp3^{WT}$ throughout regeneration, further confirming that the pancreas is positively restoring its normal, healthy state in both genotypes (Fig. 4C-D, compare with Fig. 2D-E, control). Together, these findings indicate that ELP3 in

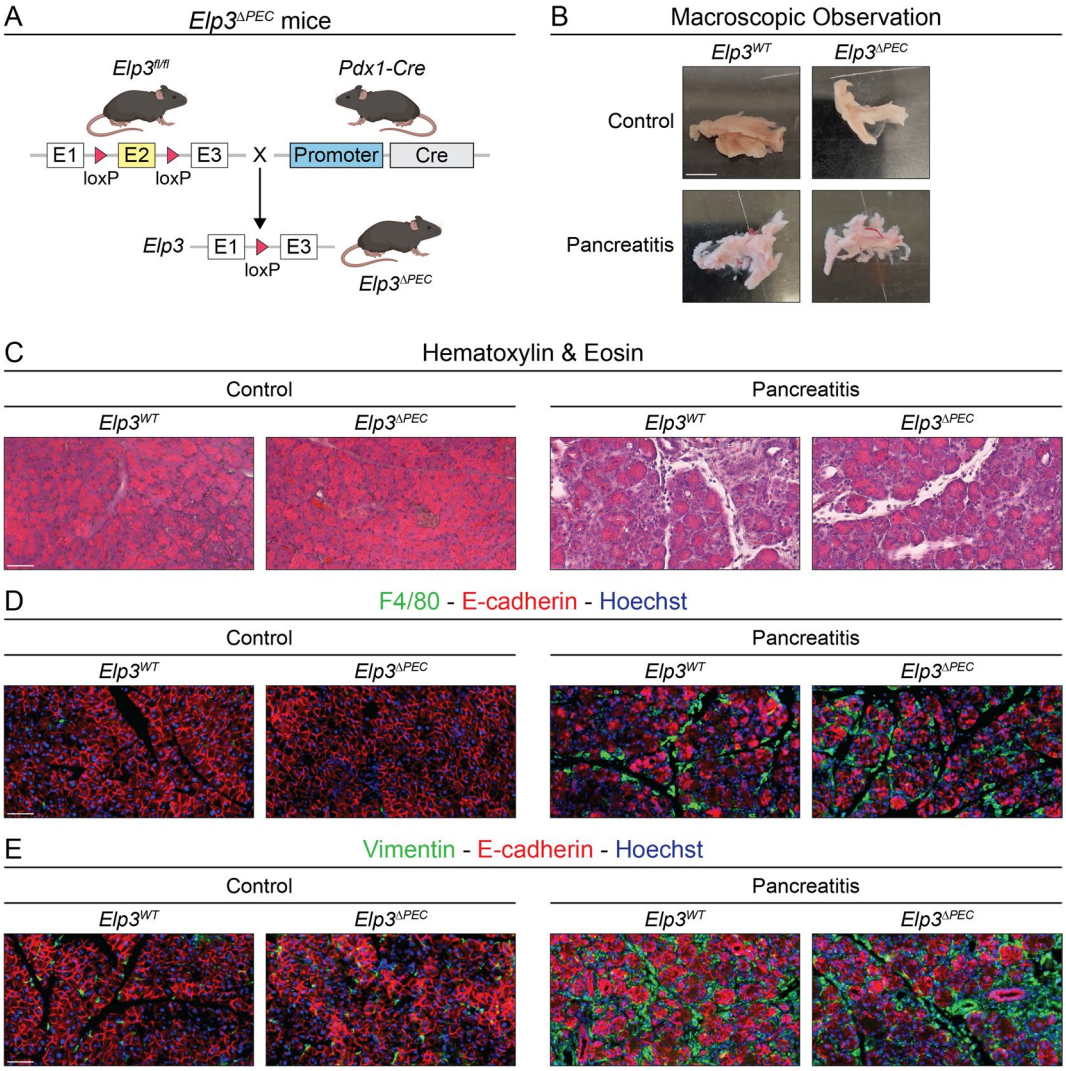

Fig. 2. Pancreatic epithelial ELP3 inactivation in the pancreas and acute pancreatitis. (**A**) Schematic representation of *Elp3* inactivation in pancreatic epithelial cells (PEC) using a floxed *Elp3* exon 2 (*Elp3-E2*) allele and Pdx1-Cre driven deletion. (**B**) Representative pancreas images from $Elp3^{WT}$ and $Elp3^{\Delta PEC}$ mice with or without caerulein treatment. Scale bar: 5 mm. (**C**) Histological staining (hematoxylin & eosin) of pancreatic sections from $Elp3^{WT}$ and $Elp3^{\Delta PEC}$ mice with or without caerulein treatment. Scale bar: 50 µm. (D-E) Immunofluorescence of F4/80 & E-cadherin (**D**) and vimentin & E-cadherin (**E**), to label macrophages (F4/80), fibroblasts (vimentin), and epithelial cells (E-cadherin), with Hoechst nuclear counterstaining, in pancreatic sections from $Elp3^{WT}$ and $Elp3^{\Delta PEC}$ mice with or without caerulein treatment. Scale bar: 50 µm.

pancreatic epithelial cells is dispensable not only for the initiation of acute pancreatitis but also for pancreatic regeneration and healing following injury.

Epithelial-specific *Elp3* inactivation is dispensable for chronic pancreatitis

Since ELP3 showed to be dispensable for both the initiation and regeneration of acute pancreatitis, we next investigated its role in chronic pancreatitis, to determine whether ELP3 might contribute under conditions of milder but sustained pancreatic injury. To this end, chronic pancreatitis was induced in C57BL/6 N mice with seven caerulein injections every other day over three-day periods each week and for three consecutive weeks (Fig. 5A). Pancreatic tissues were collected three days after the final injection (day 22), as described (Fig. 5A)[35]. In this chronic setting, the expression of U_{34}-tRNA-modifying enzymes *Elp1*, *Elp3*, *Ctu1*, and *Ctu2* remained elevated (Supplementary Fig. 2).

Histological examination with hematoxylin & eosin staining revealed no significant differences between $Elp3^{\Delta PEC}$ and $Elp3^{WT}$ mice during chronic pancreatitis (Fig. 5B). Consistently, immunofluorescence labeling of F4/80, vimentin, and E-cadherin revealed comparable levels of macrophages, fibroblasts, and epithelial density between $Elp3^{\Delta PEC}$ and $Elp3^{WT}$ in chronic pancreatitis (Fig. 5C-D). These results suggest that pancreatic epithelial ELP3 is also dispensable for chronic pancreatitis.

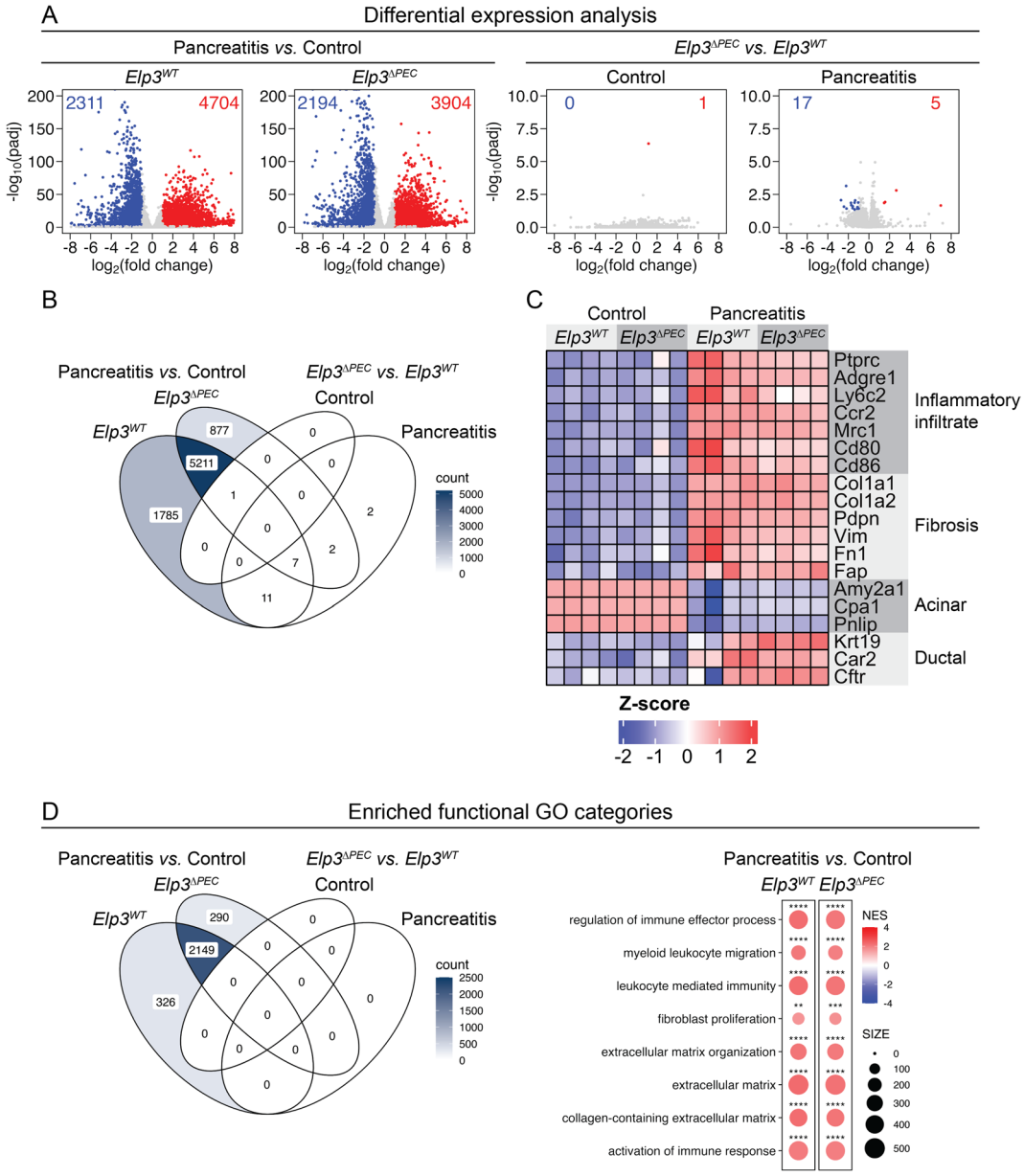

Fig. 3. Transcriptional analysis of pancreatic epithelial ELP3 inactivation in the pancreas and acute pancreatitis. (**A**) Volcano plots comparing mRNA expression in $Elp3^{WT}$ and $Elp3^{\Delta PEC}$ mice under control and acute pancreatitis conditions. Four comparisons are shown: pancreatitis vs. control in $Elp3^{WT}$ and $Elp3^{\Delta PEC}$, and $Elp3^{\Delta PEC}$ vs. $Elp3^{WT}$ in control and pancreatitis. (**B**) Venn diagram showing differentially expressed genes and overlaps across the four comparisons. (**C**) Heatmap of pancreatitis-associated genes across the four experimental groups: $Elp3^{WT}$ control, $Elp3^{\Delta PEC}$ control, $Elp3^{WT}$ pancreatitis, and $Elp3^{\Delta PEC}$ pancreatitis. (**D**) Gene Ontology (GO) enrichment analysis: Venn diagram of enriched GO terms across the four comparisons (left), and bubble plot showing enriched terms in $Elp3^{WT}$ pancreatitis vs. $Elp3^{WT}$ control, and $Elp3^{\Delta PEC}$ pancreatitis vs. $Elp3^{\Delta PEC}$ control comparisons (right). Dot size reflects gene count of the GO term. Color represents Normalized Enrichment Score (NES). Asterisks indicate statistical significance. $^{*}q < 0.05$, $^{**}q < 0.01$, $^{***}q < 0.001$, $^{****}q < 0.0001$.

Acinar-specific *Elp3* inactivation is dispensable for pancreatic cancer initiation

Given the evident lack of a clear role of pancreatic epithelial ELP3 in acute and chronic pancreatitis, we investigated its function in pancreatic tumor initiation. This is particularly relevant since ELP3 has been implicated in other cancers, including breast cancer, melanoma, and colon cancer[26–28]. Additionally, studies have shown that caerulein-induced pancreatitis accelerates pancreatic cancer development in $KRAS^{G12D}$-driven mouse models[36–39]. While ADM is typically transient and reversible in pancreatitis, it fails to resolve in $KRAS^{G12D}$-expressing acinar cells, leading to pancreatic intraepithelial neoplasia (PanIN) and accelerating

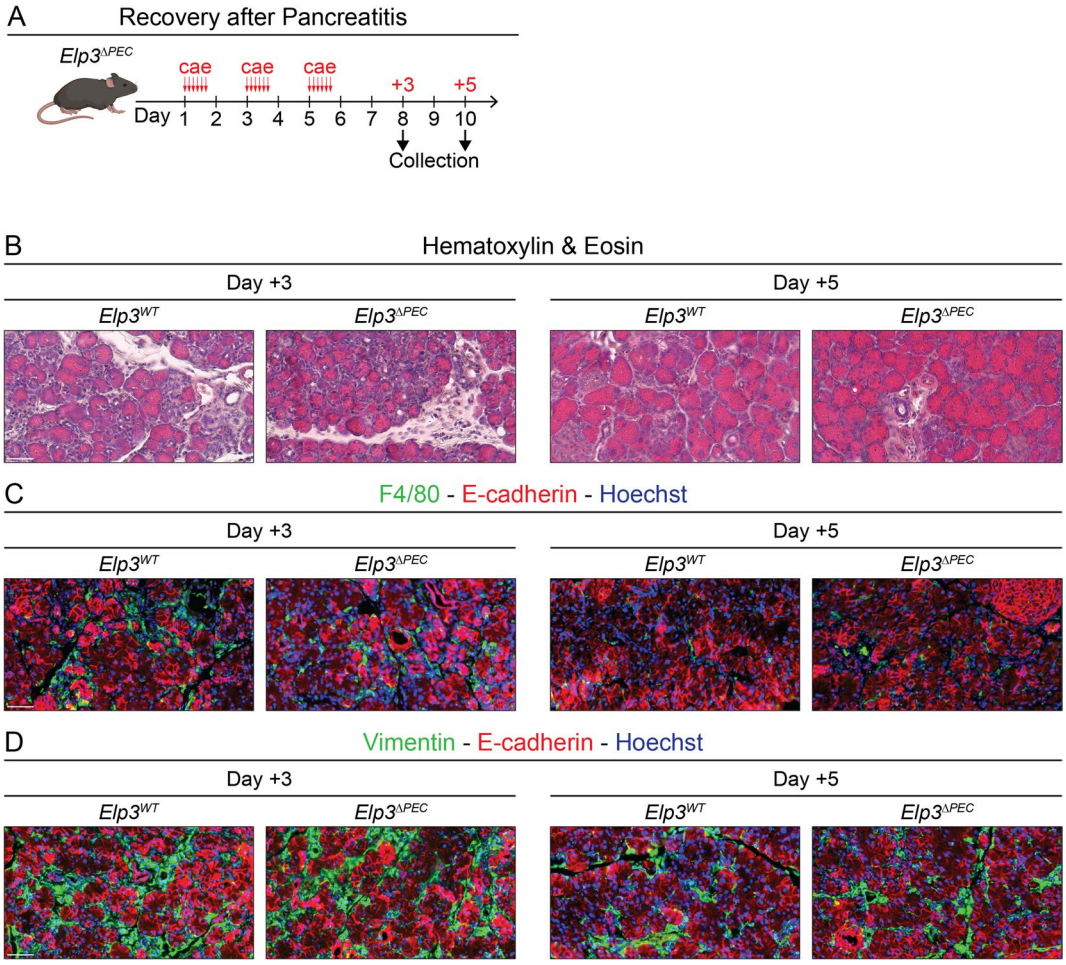

Fig. 4. Pancreatic epithelial ELP3 inactivation in regeneration post-acute pancreatitis. (**A**) Experimental timeline of acute pancreatitis induction (days 1 to 5) and regeneration showing caerulein injections and tissue collection three (day 8) and five days (day 10) after the final injection in C57BL/6 N mice. Vertical red arrows indicate the hourly injections. (**B**) Histological staining (hematoxylin & eosin) of pancreatic sections from $Elp3^{WT}$ and $Elp3^{\Delta PEC}$ mice three and five days post-acute pancreatitis. Scale bar: 50 µm. (**C,D**) Immunofluorescence of F4/80 & E-cadherin (**C**) and vimentin & E-cadherin (**D**), to label macrophages (F4/80), fibroblasts (vimentin), and epithelial cells (E-cadherin), with Hoechst nuclear counterstaining in pancreatic sections from $Elp3^{WT}$ and $Elp3^{\Delta PEC}$ mice three and five days post-acute pancreatitis. Scale bar: 50 µm.

PDAC development[37,40,41]. Thus, we hypothesized that persistent ADM in acinar cells may be influenced by ELP3, potentially regulating their transcriptome and proteome.

To explore this, we used a mouse model, the *Ptf1a-CreER*^{T2}; *Kras*$^{LSL-G12D}$, with two genetically engineered alleles, allowing acinar-specific recombination and thus activation of KRAS^{G12D} (Fig. 6A)[38]. Unlike the previously used *Pdx1-Cre* line, which drives recombination in all pancreatic epithelial cells via the Pdx1 promoter, *Ptf1a-CreERT2* uses the acinar-specific Ptf1a promoter to enable inducible and selective recombination in acinar cells, the presumed cell of origin for PDAC, as demonstrated by lineage tracing[38,42]. These mice were crossed with $Elp3^{fl/fl}$ mice to eventually generate the *Ptf1a-CreER*^{T2}; *Kras*$^{LSL-G12D}$; $Elp3^{fl/fl}$ mice, referred to as *Kras*$^{G12D-ac}$; $Elp3^{\Delta ac}$ (Fig. 6B). Tamoxifen injections triggered CreER^{T2} nuclear translocation, resulting in Cre-mediated excision of the floxed *Elp3* exon 2 (*Elp3-E2*), as performed previously with Pdx1-Cre, and of the floxed stop cassette (LSL) in *Kras*$^{LSL-G12D}$ (Fig. 6B). This simultaneously inactivated *Elp3* in acinar cells while enabling oncogenic *Kras* expression. *Kras*$^{G12D-ac}$; $Elp3^{\Delta ac}$ mice were compared with *Kras*$^{G12D-ac}$; $Elp3^{WT}$ littermates, which also express oncogenic KRAS upon tamoxifen injections but retain functional ELP3.

To induce the recombination of *Kras*^{G12D} and *Elp3* in acinar cells, tamoxifen was administered three times over five days (Fig. 6C and Supplementary Fig. 3). Two weeks later, acute pancreatitis was induced as previously described to accelerate and drive PanIN formation (Fig. 6C). Pancreata were collected ten days after the final caerulein injection (day 15; Fig. 6C). Upon PanIN induction, the expression of *Elp1*, *Elp3*, *Ctu1*, and *Ctu2* increased (Supplementary Fig. 2).

First, acute pancreatitis was induced in $Elp3^{WT}$ and $Elp3^{\Delta ac}$ mice that were wild-type for *Kras*, and pancreata were collected the day after the final injection (day 6), as previously described (Supplementary Fig. 3). Similarly

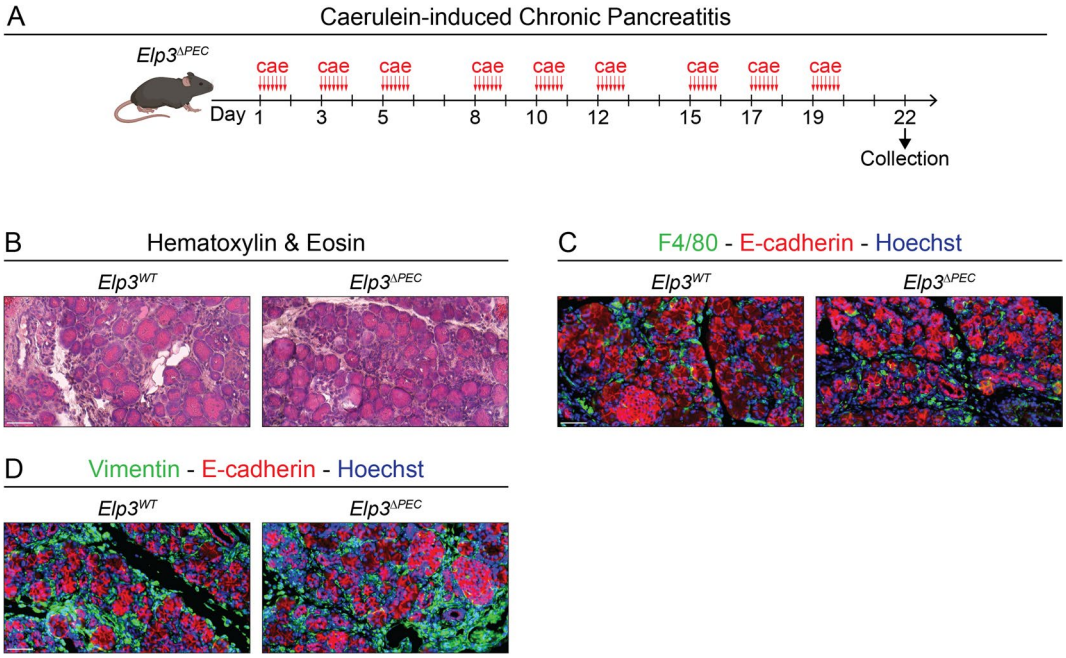

Fig. 5. Pancreatic epithelial ELP3 inactivation in chronic pancreatitis. (**A**) Experimental timeline of chronic pancreatitis showing caerulein injections over three weeks with tissue collection three days after the final injection (day 22) in C57BL/6 N mice. Vertical red arrows indicate the hourly injections. (**B**) Histological staining (hematoxylin & eosin) of pancreatic sections from $Elp3^{WT}$ and $Elp3^{\Delta PEC}$ mice under chronic pancreatitis. Scale bar: 50 µm. (**C,D**) Immunofluorescence of F4/80 & E-cadherin (**C**) and vimentin & E-cadherin (**D**), to label macrophages (F4/80), fibroblasts (vimentin), and epithelial cells (E-cadherin), with Hoechst nuclear counterstaining in pancreatic sections from $Elp3^{WT}$ and $Elp3^{\Delta PEC}$ mice under chronic pancreatitis. Scale bar: 50 µm.

to $Elp3^{\Delta PEC}$ mice, tamoxifen-induced acinar inactivation of *Elp3* had no effect on pancreatic histology following caerulein treatment (Supplementary Fig. 3), nor on macrophage or fibroblast numbers, or epithelial density (Supplementary Fig. 3). In addition, acinar-specific inactivation of *Elp3* did not alter its expression in the islets of Langerhans (Supplementary Fig. 2).

To rigorously assess the potential impact of acinar-specific *Elp3* inactivation on pancreatic cancer initiation, we systematically analyzed whole-slide scans of pancreata. In *Kras*-mutated mice, histological analysis using hematoxylin & eosin confirmed PanIN lesion induction (Fig. 6D). Unlike wild-type mice, which showed ADM regression and tissue regeneration five days after caerulein treatment (Fig. 4B), $KRAS^{G12D}$ mice exhibited persistent ADM and PanIN lesions, characterized by dramatic reduction of (acinar) eosinophilia, presence of cuboidal and columnar cells facing a lumen and surrounded by a dense stromal compartment, ten days after caerulein injections (Fig. 6D). However, $Kras^{G12D-ac}$; $Elp3^{\Delta ac}$ and $Kras^{G12D-ac}$; $Elp3^{WT}$ mice displayed similar tissue architecture and PanIN lesions (Fig. 6D). Immunofluorescence labeling of F4/80, vimentin, and E-cadherin further confirmed that PanIN lesions and tumor microenvironment were comparable in both $Kras^{G12D-ac}$; $Elp3^{\Delta ac}$ and $Kras^{G12D-ac}$; $Elp3^{WT}$ mice (Fig. 6E-F), with no significant differences observed in either the number or grade distribution of PanIN lesions. These findings suggest that acinar ELP3 is dispensable for pancreatic cancer initiation, indicating that ELP3 is not required in acinar cells undergoing persistent ADM due to the expression of oncogenic KRAS.

Discussion

In the present study, we investigated the role of ELP3 in acute and chronic pancreatitis, as well as in the initiation of pancreatic cancer. ELP3 is an acetyltransferase known to be involved in various pathological conditions related to cancer, immune regulation, and cellular differentiation, prompting us to speculate about its role in pancreatic exocrine disease. We found that ELP3 expression increased during acute pancreatitis in multiple pancreatic cell types, consistent with widespread tissue remodeling, including acinar cells which are expected to undergo ADM. We selectively inactivated ELP3 in pancreatic epithelial cells to investigate its function during acute and chronic pancreatitis, and in acinar cells to examine its role in PanIN induction. Despite these targeted approaches, ELP3 inactivation had no observable impact on pancreatic homeostasis, inflammation, regeneration, or tumor initiation. These findings, while negative, extend our understanding of ELP3's diverse, context-dependent functions beyond the pancreas and across various physiological and pathological conditions.

In situ hybridization revealed elevated *Elp3* mRNA expression primarily localized in pancreatic epithelial cells upon pancreatitis induction. This upregulation of ELP3 may be linked to ADM, a process through which acinar cells acquire ductal-like characteristics at the transcriptomic, proteomic, and cytological levels. This

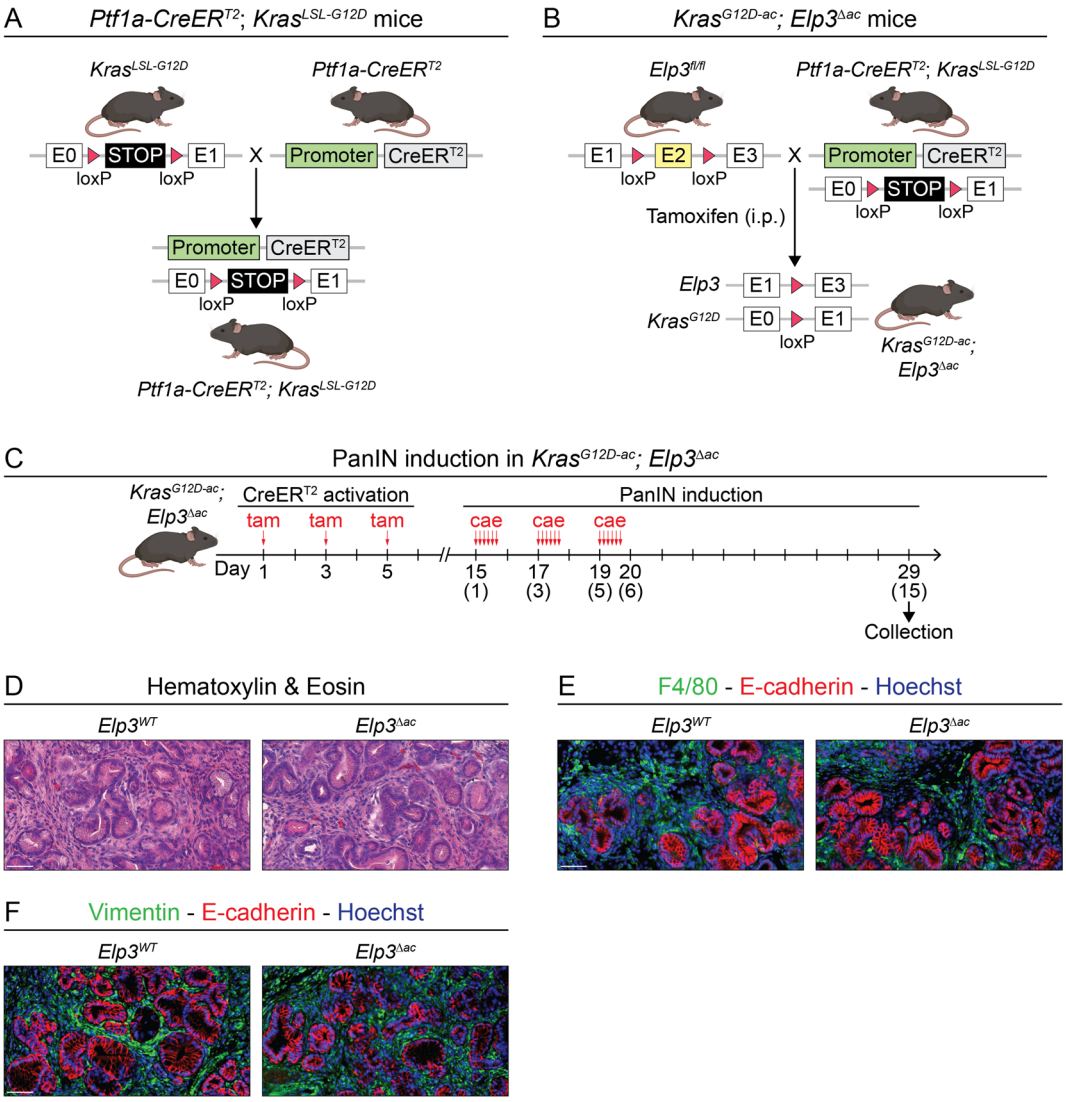

Fig. 6. Acinar ELP3 inactivation in pancreatic intraepithelial neoplasia (PanIN) induction. (**A**) Schematic representation of *Ptf1a-CreER*^{T2}; *Kras*$^{LSL-G12D}$ model. (**B**) strategy for generating *Kras*$^{G12D-ac}$; *Elp3*$^{\Delta ac}$ mice. (**C**) Experimental timeline of tamoxifen and caerulein administration, with tissue collection ten days post-treatment (day 15). (**D**) Histological staining (hematoxylin & eosin) of pancreatic sections from *Kras*$^{G12D-ac}$; *Elp3*$^{\Delta ac}$ (*Elp3*$^{\Delta ac}$) and *Kras*$^{G12D-ac}$; *Elp3*^{WT} (*Elp3*^{WT}) mice. Scale bar: 50 µm. (**E,F**) Immunofluorescence of F4/80 & E-cadherin (**E**) and vimentin & E-cadherin (**F**), to label macrophages (F4/80), fibroblasts (vimentin), and epithelial cells (E-cadherin), with Hoechst nuclear counterstaining in pancreatic sections from *Kras*$^{G12D-ac}$; *Elp3*$^{\Delta ac}$ (*Elp3*$^{\Delta ac}$) and *Kras*$^{G12D-ac}$; *Elp3*^{WT} (*Elp3*^{WT}) mice. Scale bar: 50 µm.

increased *Elp3* expression was also observed by RT-qPCR, and was extended to *Elp1*, *Ctu1*, and *Ctu2* mRNAs, all involved in wobble uridine tRNA modifications. While these results support the in situ hybridization data and indicate that *Elp3* and its associated partners are upregulated in the pancreas during ADM, we cannot rule out the possibility that the increased expression measured by RT-qPCR also stems from non-epithelial cells in the inflamed pancreas. Among these, macrophages are a prominent population in acute pancreatitis[8]. Notably, in the colon, macrophages upregulate ELP3 upon alternative polarization[32]. Consistent with publicly available single-cell RNA sequencing data (Supplementary Fig. 2), we also detected *Elp3* expression in macrophages and fibroblasts (Supplementary Fig. 2).

To inactivate ELP3, we used the Pdx1-Cre mice, which have been widely used to investigate the function of genes during embryonic development and in adult tissues. Despite the early *Elp3* inactivation in pancreatic progenitors, and thus in all the pancreatic epithelial lineages, *Elp3*-knockout pancreata displayed normal size, shape, histology, and transcriptome as compared to wild-type control pancreata at two months of age. This indicates that ELP3 is not involved in pancreas development, nor in pancreas homeostasis. Importantly, this lack of phenotype is not explained by compensation from other Elongator subunits. The Elongator complex is a tightly interdependent hexamer (ELP1–ELP6), with ELP3 serving as the sole catalytic subunit responsible for tRNA modification[43]. Because Elongator function strictly requires ELP3, expression of other subunits does

not provide functional compensation for ELP3 loss. Regardless, no upregulation of any Elongator complex subunit (ELP1-ELP6) or of CTU1/CTU2 was observed in *Elp3*$^{\Delta PEC}$ pancreata under either control or pancreatitis conditions.

In adult control pancreata, *Elp3* mRNA was detected by in situ hybridization only in the endocrine compartment, suggesting that ELP3 may have minimal expression and activity in the adult exocrine pancreas. However, this lack of ELP3 function in pancreatic homeostasis mirrors observations from the intestine, where ELP3 was similarly dispensable for overall intestinal homeostasis[32].

Furthermore, ELP3 appeared non-essential in acute and chronic pancreatitis, as shown by bulk RNA sequencing in acute pancreatitis and histological analyses in both models. These results suggest that ELP3 is not required for pancreatitis-associated ADM, and ductal-like cells do not depend on ELP3, in contrast to intestinal tuft cells, T follicular helper cells, cortical neuron development, and committing progenitors in hematopoiesis[26,29–31,44]. One explanation could be that ductal-like cells, a progenitor-like cell type, have relatively low protein synthesis and NAA codon usage, reducing their reliance on ELP3. For instance, committing progenitors require ELP3 due to their high protein synthesis or metabolic activity, whereas long-term hematopoietic stem cells, which have lower activity, do not[29]. It is also possible that while ELP3 may regulate the translation of NAA-enriched mRNAs in ductal-like cells, none of its targets are critical in pancreatitis. For instance, although ELP3 drives intestinal cancer initiation by regulating SOX9 translation in an NAA-dependent manner[26], SOX9 is dispensable in acinar cells during pancreatitis[38]. Moreover, it is possible that acinar cells bypass the effects of ELP3 inactivation. These exocrine glandular cells continuously produce zymogens and require a high translational capacity. Elevated UUN-tRNA levels can counteract the effects of Elongator depletion[21], suggesting that highly translational acinar cells may be inherently resilient to ELP3 inactivation.

ELP3 inactivation in acinar cells did not affect pancreatic tumor initiation, as PanIN lesions developed despite the absence of ELP3. Unlike in the intestine, the pancreas may lack a subpopulation of stem cells dependent on ELP3 for cancer initiation[26]. Alternatively, PDAC might rely on ELP3 at later stages of tumor progression. Other cancers show a dependency on ELP3 for distinct hallmarks: breast cancer relies for invasion and metastasis[27], and melanoma for resistance to anti-BRAF therapy[28]. In human pancreatic cancer cells, ELP3 has been identified as a collateral dependency of oncogenic KRAS inhibition, with CRISPR-mediated knockout sensitizing cells to KRAS inhibition[45].

Lastly, we cannot rule out a role for non-acinar ELP3 in pancreatitis and pancreatic cancer initiation. Non-epithelial *Elp3* expression could be observed in our in situ hybridization data from *Elp3*$^{\Delta PEC}$ pancreata during pancreatitis (Supplementary Fig. 1), indicating that *Elp3* expression in non-epithelial cells remained unaffected between *Elp3*^{WT} and *Elp3*$^{\Delta PEC}$ mice, as expected given the epithelial specificity of Pdx1-Cre. Given the link between pancreatitis and pancreatic cancer, ELP3 in macrophages could influence PanIN formation by modulating inflammation. In the colon, macrophage-derived ELP3 not only attenuates inflammation but also delays tumor initiation[32]. These observations, together with our findings, highlight the importance of considering ELP3's functions beyond the epithelial compartment. Given the broad and context-dependent roles of ELP3 across tissues, this study used targeted knockouts in pancreatic epithelial and acinar cells to investigate its function in well-established models of pancreatitis and tumor initiation. Our findings clarify that both the initiation and recovery of pancreatitis, as well as PanIN formation, occur independently of ELP3 in epithelial and acinar cells. These results refine our understanding of ELP3's tissue-specific functions and open new avenues for exploring its role in other cell types, such as macrophages, that may influence pancreatic disease.

Methods

Ethics statement

Mice were maintained in individually ventilated cages (IVC) under standard laboratory conditions. Animal care and experimental procedures were conducted in accordance with the European 2010/63/EU directive on the protection of animals used for scientific purposes, followed the recommendations of the ARRIVE guidelines, and were authorized and approved by the UCLouvain Animal Ethics Committee (2020/UCL/MD/011 and 2023/UCL/MD/47).

Mice and treatments

Wild-type mice of C57BL/6 N strain were obtained from Charles River Laboratories. Mouse lines have been described previously, *Elp3*$^{loxp/loxp}$[26], or were provided by collaborators, Tg(*Ipf1-Cre*$^{1Tuv/Nci}$) mice from Francesca Spagnoli[46,47], Tg(*Ptf1a*$^{Cre\ -\ ERTM}$) mice from Chris Wright[48] via Francisco X. Real, and Tg(*Kras*$^{LSL-G12D}$) from Patrick Jacquemin (UCLouvain, Brussels, Belgium).

To generate pancreatic epithelial cell *Elp3* knockout (*Elp3*$^{\Delta PEC}$) mice, male hemizygous *Pdx1-Cre* (Tg(*Ipf1-Cre*$^{1Tuv/Nci}$)) mice were bred with female *Elp3*$^{fl/fl}$ (Tg(*Elp3*$^{loxp/loxp}$)) mice to obtain *Pdx1-Cre; Elp3*$^{fl/+}$. The latter were crossed with *Elp3*$^{fl/fl}$ to generate *Elp3*$^{\Delta PEC}$ (*Pdx1-Cre; Elp3*$^{fl/fl}$) mice and their wild-type littermates (*Elp3*^{WT}), which lacked the *Pdx1-Cre* transgene. All mice were maintained on a C57BL/6 N background.

For acinar cell *Elp3* knockout with oncogenic KRAS^{G12D} expression (*Kras*$^{G12D-ac}$; *Elp3*$^{\Delta ac}$), male hemizygous *Ptf1a-CreER*^{T2}; *Kras*$^{LSL-G12D}$ (Tg(*Ptf1a*$^{Cre-ERTM}$); Tg(*Kras*$^{LSL-G12D}$)) were crossed with female *Elp3*$^{fl/fl}$ mice. The resulting progeny included *Kras*$^{G12D-ac}$; *Elp3*$^{\Delta ac}$ mice (*Ptf1a-CreER*^{T2}; *Kras*$^{LSL-G12D}$; *Elp3*$^{fl/fl}$) and their wild-type littermates with oncogenic *Kras* expression (*Kras*$^{G12D-ac}$; *Elp3*^{WT}). To induce nuclear translocation of CreER^{T2} and acinar-specific recombination of *Elp3* floxed exon 2 (*Elp3*$^{fl/fl}$) and of *Kras* floxed stop cassette (*Kras*$^{LSL-G12D}$), tamoxifen (T5648, Sigma-Aldrich) was dissolved in corn oil at 25 mg/mL, and administered intraperitoneally at 125 µg/g body weight on days 1, 3, and 5. Mice were allowed to rest for one week before subsequent experimentation.

Acute pancreatitis
6-8-week-old wild-type C57BL/6N, *Elp3*$^{\Delta PEC}$, and *Elp3*^{WT} mice, were administered caerulein (AS-24252, Eurogentec) dissolved in sterile phosphate-buffered saline (PBS) at 37.5 µg/mL. Six intraperitoneal injections at 125 µg/kg body weight were given hourly, every 48 h over three sessions. The pancreas was collected either one day after the final injection, or at three and five days for regeneration studies.

Chronic pancreatitis
6-8-week-old *Elp3*$^{\Delta PEC}$ and *Elp3*^{WT} mice received seven hourly intraperitoneal injections at 50 µg/kg body weight, administered every 48 h over three weekly sessions, in three consecutive weeks. The pancreas was harvested three days post-final injection.

PanIN
6-8-week-old *Kras*$^{G12D-ac}$; *Elp3*$^{\Delta ac}$ and *Kras*$^{G12D-ac}$; *Elp3*^{WT} mice received six hourly intraperitoneal caerulein injections at 75 µg/kg body weight, repeated every 48 h over three sessions. Pancreatic tissue was collected ten days following the final injection.

Histology, mRNA in situ hybridization, immunofluorescence, and microscopy
Tissue processing
Pancreatic tissues were fixed overnight at 4 °C in 4% paraformaldehyde diluted in PBS. The following day, tissues underwent dehydration and paraffin embedding with a Tissue-Tek VIP-6 (Sakura). Sections were then cut at a thickness of 6 µm for histological and immunofluorescence analysis.

Histological staining
Paraffin-embedded sections were deparaffinized and stained either with hematoxylin & eosin (H&E) to distinguish nuclei (hematoxylin) from the cytoplasm and extracellular matrix (eosin), or sirius red/fast green to differentiate collagen (sirius red) from cytoplasmic proteins (fast green).

mRNA in situ hybridization
To detect *Elp3* and *Elp3-E2* mRNAs, deparaffinized sections were processed using the RNAscope™ 2.5 HD Assay – RED with the Mm-Elp3-10zz-O1-C1-Mm probe (1240521-C1) for *Elp3* mRNA, or the BaseScope™ RED Assay with the BA-Mm-Elp3-E2-1zz-st-C1-Mm (1300821-C1). Experiments were conducted following the instructions of the manufacturer and as previously described[49]. After hybridization, slides underwent immunofluorescence colabeling (see below), starting from the blocking step.

Immunofluorescence
The immunolabeling and imaging were conducted as previously described[47,49–51]. Deparaffinized sections underwent antigen retrieval by boiling in 10mM sodium citrate (pH = 6.0), in a microwave at 750 W, for 5 min, twice. Permeabilization was then performed at room temperature for 5 min in a PBS solution with 0.3% Triton X-100. Blocking was carried out for 45 min at room temperature using PBS supplemented with 0.3% Triton X-100, 10% bovine serum albumin (BSA), and 3% milk. Primary antibodies were diluted in the blocking solution and incubated with the sections overnight at 4 °C. The next day, sections were washed three times with PBS supplemented with 0.1% Triton X-100 and then further incubated for 1 h at room temperature with secondary antibodies and the nuclear counterstain Hoechst 33,342 at 250 ng/mL, both diluted in PBS supplemented with 0.3% Triton X-100 and 10% bovine serum albumin (BSA). Sections were washed twice with PBS supplemented with 0.1% Triton X-100 and once with distilled water before mounting.

Antibodies
Primary antibodies: anti-E-cadherin (mouse IgG2a, 1:250, 610182, BD), anti-F4/80 (rabbit, 1:250, 70076, Cell Signaling), anti-vimentin (rabbit, 1:100, 5741, Cell Signaling). Secondary antibodies: Goat anti-Mouse IgG2a (Alexa Fluor™ 568, 1:500, A21134, Invitrogen), Goat anti-Rabbit IgG (Alexa Fluor™ 488, 1:500, A11034, Invitrogen).

Mounting
Slides were coverslipped with Dako Faramount Aqueous Mounting Medium (Agilent Technologies, Santa Clara, CA, USA).

Microscopy and imaging
All stained and immunolabelled sections were scanned using a Pannoramic 250 Flash III digital slide scanner (3DHistech) to generate high-resolution whole-slide images. Histological analyses were performed on the entire tissue section using these scans to ensure consistent and unbiased evaluation across samples. Representative fields were selected from the whole-slide images for display in the figures. Image selection and quantitative analyses were conducted by investigators blinded to group identity.

RNA isolation, RT-qPCR, and RNA sequencing
RNA isolation
Small pancreatic tissue samples, measuring 2 × 2 mm, were carefully dissected, and immersed in RNAlater™ Stabilization Solution (AM7021, Invitrogen) to preserve RNA integrity. The samples were then snap-frozen in liquid nitrogen for preservation. For RT-qPCR, total RNA was isolated with the ReliaPrep™ RNA Miniprep System (Z6111, Promega). The manufacturer's protocol for ≤ 5 mg fibrous tissues was employed. For RNA

sequencing, total RNA was isolated using TriPure Isolation Reagent (11667157001, Roche) and RNA integrity was analyzed using Agilent 2100 Bioanalyzer and Agilent RNA 6000 Nano Assay (Agilent Technologies).

RT-qPCR

500ng of total RNA were used for reverse transcription, along with random hexamers and the M-MLV Reverse Transcriptase (28025013, Invitrogen). The synthesized cDNA was then subjected to quantitative PCR (qPCR) using KAPA SYBR® FAST qPCR Master Mix (2X) (KK4602, Roche), and primer pairs specific to the target cDNA. The $2^{-\Delta\Delta Ct}$ method was employed to compare gene expression levels, normalized to *18 S* ribosomal RNA as the housekeeping reference. The resulting fold changes in expression were log2-transformed and displayed in the graphs.

Primer pairs: *18S* 5'-GTAACCCGTTGAACCCCATT-3' and 5'-CCATCCAATCGGTAGTAGCG-3', *Elp1* 5'-TCTGCAATCTCAGCACACAG-3' and 5'-GGACTCCAGCTCATGACAGA-3', *Elp3* 5'-GCTGAGCTGATGATGCTGAC-3' and 5'-ACGTCTTTCCCCTGCTCAT-3', *Ctu1* 5'-CATGAACTTCCTGCGTGGT-3' and 5'-CGCACTCCTCGGAAAAGTAG-3', *Ctu2* 5'-GAGAAGGTGCTCCTGTCCTG-3' and 5'-CTGTCCTCCAAGCTCTGACC-3'.

RNA sequencing

RNA libraries were prepared using the Illumina Stranded Total RNA Prep with Ribo-Zero Plus, following the manufacturer's instructions. Library quantification and normalization were performed via qPCR using the KAPA Library Quantification Kit (Sopachem). Sequencing was carried out on the NovaSeq 6000 in paired-end mode with 150 cycles, generating 50 million paired-end reads per sample. Raw sequencing reads were demultiplexed and adapter-trimmed using Illumina bcl2fastq v2.20. Data processing was performed using custom Nextflow RNA-seq pipeline, adapted from nf-core/rnaseq. Reads underwent quality filtering with TrimGalore[52], which removed poly-G tails and performed quality-based trimming, including the removal of a single base from both the 5' and 3' ends. Read alignment was performed using STAR[53], against the Mus musculus reference genome (GRCm39) with annotations from Ensembl release 107. Gene-level quantification was conducted using Salmon[54]. Throughout the pipeline, various quality control (QC) steps were applied, with results consolidated into a final MultiQC report. Differential expression analysis was performed using DESeq2[55].

Single-cell RNA sequencing data

Single-cell RNA sequencing data from acute pancreatitis (GSE235874 and GSE188819) were analyzed. The analysis of GSE235874, including normalized expression over time for epithelial subsets (acinar, ADM, and ductal) and combined acinar/ADM populations, was performed as previously described[34]. The GSE188819 dataset was used separately to visualize all cell types present in pancreatitis[56].

Statistical analysis

Data analysis and presentation were performed using GraphPad Prism for RT-qPCR and RStudio for RNA sequencing. For RT-qPCR, statistical analysis was conducted using a two-tailed Student's t-test, after verifying that the data met the criteria for homoscedasticity and normality. Homoscedasticity was assessed using Spearman's test for heteroscedasticity, while normality was evaluated with both the Shapiro-Wilk and D'Agostino-Pearson omnibus (K2) tests. Statistical significance was set at $p < 0.05$.

Data availability

RNA sequencing data have been deposited in the Gene Expression Omnibus (GEO) under accession number GSE296464.

Received: 17 April 2025; Accepted: 1 October 2025
Published online: 06 November 2025

References

1. Gerasimenko, J. V., Gerasimenko, O. V. & Petersen, O. H. The role of Ca2 + in the pathophysiology of pancreatitis. *J. Physiol.* **592**, 269 (2013).
2. Li, J., Zhou, R., Zhang, J. & Li, Z. F. Calcium signaling of pancreatic acinar cells in the pathogenesis of pancreatitis. *World J. Gastroenterol.* **20**, 16146–16152 (2014).
3. Lerch, M. M. & Gorelick, F. S. Models of acute and chronic pancreatitis. *Gastroenterology* **144**, 1180–1193 (2013).
4. Forsmark, C. E., Vege, S. S. & Wilcox, C. M. Acute pancreatitis. *N Engl. J. Med.* **375**, 1972–1981 (2016).
5. Patra, P. S. & Das, K. Longer-term outcome of acute pancreatitis: 5 years follow-up. *JGH Open.* **5**, 1323–1327 (2021).
6. Van Laethem, J., Robberecht, P., Resibois, A. & Deviere, J. Transforming growth factor beta promotes development of fibrosis after repeated courses of acute pancreatitis in mice. *Gastroenterology* **110**, 576–582 (1996).
7. Hegyi, P. J. et al. Evidence for diagnosis of early chronic pancreatitis after three episodes of acute pancreatitis: a cross-sectional multicentre international study with experimental animal model. *Sci. Rep.* **11**, 1367 (2021).
8. Liou, G. Y. et al. Macrophage-secreted cytokines drive pancreatic acinar-to-ductal metaplasia through NF-κB and MMPs. *J. Cell. Biol.* **202**, 563–577 (2013).
9. Klöppel, G. & Maillet, B. The morphological basis for the evolution of acute pancreatitis into chronic pancreatitis. *Virchows Arch. A.* **420**, 1–4 (1992).
10. Stanger, B. Z. & Hebrok, M. Control of cell identity in pancreas development and regeneration. *Gastroenterology* **144**, 1170–1179 (2013).
11. Pinho, A. V. et al. Adult pancreatic acinar cells dedifferentiate to an embryonic progenitor phenotype with concomitant activation of a senescence programme that is present in chronic pancreatitis. *Gut* **60**, 958–966 (2011).
12. Schlesinger, Y. et al. Single-cell transcriptomes of pancreatic preinvasive lesions and cancer reveal acinar metaplastic cells' heterogeneity. *Nat. Commun.* **11**, 4516 (2020).
13. Hawkes, N. A. et al. Purification and characterization of the human elongator Complex *. *J. Biol. Chem.* **277**, 3047–3052 (2002).

14. Winkler, G. S. et al. RNA polymerase II elongator holoenzyme is composed of two discrete Subcomplexes *. *J. Biol. Chem.* **276**, 32743–32749 (2001).
15. Krogan, N. J. & Greenblatt, J. F. Characterization of a Six-Subunit Holo-Elongator complex required for the regulated expression of a group of genes in Saccharomyces cerevisiae. *Mol. Cell. Biol.* **21**, 8203–8212 (2001).
16. Fellows, J., Erdjument-Bromage, H., Tempst, P. & Svejstrup, J. Q. The Elp2 subunit of elongator and elongating RNA polymerase II holoenzyme is a WD40 repeat Protein *. *J. Biol. Chem.* **275**, 12896–12899 (2000).
17. Otero, G. et al. Elongator, a multisubunit component of a novel RNA polymerase II holoenzyme for transcriptional elongation. *Mol. Cell.* **3**, 109–118 (1999).
18. Wittschieben, B. Ø., Fellows, J., Du, W., Stillman, D. J. & Svejstrup, J. Q. Overlapping roles for the histone acetyltransferase activities of SAGA and elongator in vivo. *EMBO J.* **19**, 3060–3068 (2000).
19. Winkler, G. S., Kristjuhan, A., Erdjument-Bromage, H., Tempst, P. & Svejstrup, J. Q. Elongator is a histone H3 and H4 acetyltransferase important for normal histone acetylation levels in vivo. *Proc. Natl. Acad. Sci.* **99**, 3517–3522 (2002).
20. Holmberg, C. et al. A novel specific role for IκB kinase Complex-associated protein in cytosolic stress signaling*. *J. Biol. Chem.* **277**, 31918–31928 (2002).
21. Esberg, A., Huang, B., Johansson, M. J. O. & Byström, A. S. Elevated levels of two tRNA species bypass the requirement for elongator complex in transcription and exocytosis. *Mol. Cell.* **24**, 139–148 (2006).
22. Creppe, C. et al. Elongator controls the migration and differentiation of cortical neurons through acetylation of α-tubulin. *Cell* **136**, 551–564 (2009).
23. Even, A. et al. ATP-citrate lyase promotes axonal transport across species. *Nat. Commun.* **12**, 5878 (2021).
24. Lin, T. Y. et al. The elongator subunit Elp3 is a non-canonical tRNA acetyltransferase. *Nat. Commun.* **10**, 625 (2019).
25. Nedialkova, D. D. & Leidel, S. A. Optimization of codon translation rates via tRNA modifications maintains proteome integrity. *Cell* **161**, 1606–1618 (2015).
26. Ladang, A. et al. Elp3 drives Wnt-dependent tumor initiation and regeneration in the intestine. *J. Exp. Med.* **212**, 2057–2075 (2015).
27. Delaunay, S. et al. Elp3 links tRNA modification to IRES-dependent translation of LEF1 to sustain metastasis in breast cancer. *J. Exp. Med.* **213**, 2503–2523 (2016).
28. Rapino, F. et al. Codon-specific translation reprogramming promotes resistance to targeted therapy. *Nature* **558**, 605–609 (2018).
29. Rosu, A. et al. Loss of tRNA-modifying enzyme Elp3 activates a p53-dependent antitumor checkpoint in hematopoiesis. *J. Exp. Med.* **218**, e20200662 (2021).
30. Lemaitre, P. et al. Loss of the transfer RNA wobble uridine–modifying enzyme Elp3 delays T cell cycle entry and impairs T follicular helper cell responses through deregulation of Atf4. *J. Immunol.* **206**, 1077–1087 (2021).
31. Wathieu, C. et al. Loss of Elp3 blocks intestinal tuft cell differentiation via an mTORC1-Atf4 axis. *EMBO J.* **43**, 3916–3947 (2024).
32. Chen, D. et al. Elp3-mediated codon-dependent translation promotes mTORC2 activation and regulates macrophage polarization. *EMBO J.* **41**, e109353 (2022).
33. Xue, J. et al. Alternatively activated macrophages promote pancreatic fibrosis in chronic pancreatitis. *Nat. Commun.* **6**, 7158 (2015).
34. Aney, K. J. et al. Novel approach for pancreas transcriptomics reveals the cellular landscape in homeostasis and acute pancreatitis. *Gastroenterology* **166**, 1100–1113 (2024).
35. Lee, K. E., Spata, M., Maduka, R., Vonderheide, R. H. & Simon, M. C. Hif1α deletion limits tissue regeneration via aberrant B cell accumulation in experimental pancreatitis. *Cell. Rep.* **23**, 3457–3464 (2018).
36. Carrière, C., Young, A. L., Gunn, J. R., Longnecker, D. S. & Korc, M. Acute pancreatitis markedly accelerates pancreatic cancer progression in mice expressing oncogenic Kras. *Biochem. Biophys. Res. Commun.* **382**, 561–565 (2009).
37. Morris, J. P., Cano, D. A., Sekine, S., Wang, S. C. & Hebrok, M. β-catenin blocks Kras-dependent reprogramming of acini into pancreatic cancer precursor lesions in mice. *J. Clin. Invest.* **120**, 508–520 (2010).
38. Kopp, J. L. et al. Identification of Sox9-dependent acinar-to-ductal reprogramming as the principal mechanism for initiation of pancreatic ductal adenocarcinoma. *Cancer Cell.* **22**, 737–750 (2012).
39. Assi, M. et al. Dynamic regulation of expression of KRAS and its effectors determines the ability to initiate tumorigenesis in pancreatic acinar cells. *Cancer Res.* **81**, 2679–2689 (2021).
40. Jensen, J. N. et al. Recapitulation of elements of embryonic development in adult mouse pancreatic regeneration. *Gastroenterology* **128**, 728–741 (2005).
41. O, J. P. D. L. & Murtaugh, L. C. Notch and Kras in pancreatic cancer: at the crossroads of mutation, differentiation and signaling. *Cell. Cycle*. https://doi.org/10.4161/cc.8.12.8744 (2009).
42. Houbracken, I. et al. Lineage tracing evidence for transdifferentiation of acinar to duct cells and plasticity of human pancreas. *Gastroenterology* **141**, 731–741e4 (2011).
43. Dalwadi, U. & Yip, C. K. Structural insights into the function of elongator. *Cell. Mol. Life Sci.* **75**, 1613–1622 (2018).
44. Laguesse, S. et al. A dynamic unfolded protein response contributes to the control of cortical neurogenesis. *Dev. Cell.* **35**, 553–567 (2015).
45. Lou, K. et al. KRASG12C inhibition produces a driver-limited state revealing collateral dependencies. *Sci. Signal.* **12**, eaaw9450 (2019).
46. Hingorani, S. R. et al. Preinvasive and invasive ductal pancreatic cancer and its early detection in the mouse. *Cancer Cell.* **4**, 437–450 (2003).
47. Glorieux, L. et al. Development of a 3D atlas of the embryonic pancreas for topological and quantitative analysis of heterologous cell interactions. *Development* **149**, dev199655 (2022).
48. Pan, F. C. et al. Spatiotemporal patterns of multipotentiality in Ptf1a-expressing cells during pancreas organogenesis and injury-induced facultative restoration. *Development* **140**, 751–764 (2013).
49. Heymans, C. et al. Spatio-temporal expression pattern and role of the tight junction protein MarvelD3 in pancreas development and function. *Sci. Rep.* **11**, 14519 (2021).
50. Glorieux, L. et al. In-depth analysis of the pancreatic extracellular matrix during development for next-generation tissue engineering. *Int. J. Mol. Sci.* **24**, 10268 (2023).
51. Moulis, M. et al. Identification and implication of tissue-enriched ligands in epithelial–endothelial crosstalk during pancreas development. *Sci. Rep.* **12**, 12498 (2022).
52. Krueger, F. Trim Galore! A wrapper around Cutadapt and FastQC to consistently apply adapter and quality trimming to FastQ files, with extra functionality for RRBS data. *Babraham Inst.* (2015). https://cir.nii.ac.jp/crid/137029464376292969.
53. Dobin, A. et al. STAR: ultrafast universal RNA-seq aligner. *Bioinformatics* **29**, 15–21 (2013).
54. Patro, R., Duggal, G., Love, M. I., Irizarry, R. A. & Kingsford, C. Salmon provides fast and bias-aware quantification of transcript expression. *Nat. Methods*. **14**, 417–419 (2017).
55. Love, M. I., Huber, W. & Anders, S. Moderated estimation of fold change and dispersion for RNA-seq data with DESeq2. *Genome Biol.* **15**, 550 (2014).
56. Melendez, E. et al. Natural killer cells act as an extrinsic barrier for in vivo reprogramming. *Development* **149**, dev200361 (2022).

Acknowledgements

The authors would like to thank Francesca Spagnoli for supplying the Pdx1-Cre mice, and Francisco X. Real/

Chris Wright for providing the Ptf1a-CreERT2 mice, as well as Bérénice Lossignol and Jonathan Decarpentrie for their support to the project.

Author contributions

Conceptualization: E.A., P.C. and C.E.P.; formal analysis: E.A., P.C. and C.E.P.; investigation: E.A., H.L., S.M., M.L.; resources: K.J.A., S.H., A.C., L.N., P.H., D.T., P.C. and C.E.P.; writing—original draft preparation: E.A., P.C. and C.E.P.; supervision: P.C. and C.E.P.; funding acquisition: E.A., P.C. and C.E.P. All authors have read and agreed to the published version of the manuscript.

Declarations

Competing interests

The authors declare no competing interests.

Additional information

Supplementary Information The online version contains supplementary material available at https://doi.org/10.1038/s41598-025-22849-8.

Correspondence and requests for materials should be addressed to E.A., P.C. or C.E.P.

Reprints and permissions information is available at www.nature.com/reprints.

Publisher's note Springer Nature remains neutral with regard to jurisdictional claims in published maps and institutional affiliations.